Experimental Neurology 317 (2019) 87–99

Contents lists available at ScienceDirect

Experimental Neurology

journal homepage: www.elsevier.com/locate/yexnr

Research paper

Repetitive closed-head impact model of engineered rotational acceleration (CHIMERA) injury in rats increases impulsivity, decreases dopaminergic innervation in the olfactory tubercle and generates white matter inflammation, tau phosphorylation and degeneration

Cole Vonder Haar[a,b,1], Kris M. Martens[a,b,1], Asma Bashir[b,1], Kurt A. McInnes[c], Wai Hang Cheng[b], Honor Cheung[b], Sophie Stukas[b], Carlos Barron[b], Tessa Ladner[b], Kassandra A. Welch[b], Peter A. Cripton[c], Catharine A. Winstanley[b], Cheryl L. Wellington[b,*]

[a] Injury and Recovery Laboratory, Department of Psychology, West Virginia University, Morgantown, WV 26508, USA
[b] Djavad Mowafaghian Centre for Brain Health, University of British Columbia, Vancouver, BC V6T 1Z3, Canada
[c] International Centre On Repair Discoveries, Department of Mechanical Engineering, University of British Columbia, Vancouver, BC V5Z 1M9, Canada

ARTICLE INFO

Keywords:
CHIMERA
Repetitive TBI
Impulsivity
Reward circuitry
White matter inflammation
Corpus callosum degeneration
Tau phosphorylation

ABSTRACT

Traumatic brain injury (TBI) affects at least 3 M people annually. In humans, repetitive mild TBI (rmTBI) can lead to increased impulsivity and may be associated with chronic traumatic encephalopathy. To better understand the relationship between repetitive TBI (rTBI), impulsivity and neuropathology, we used CHIMERA (Closed-Head Injury Model of Engineered Rotational Acceleration) to deliver five TBIs to rats, which were continuously assessed for trait impulsivity using the delay discounting task and for neuropathology at endpoint. Compared to sham controls, rats with rTBI displayed progressive impairment in impulsive choice. Histological analyses revealed reduced dopaminergic innervation from the ventral tegmental area to the olfactory tubercle, consistent with altered impulsivity neurocircuitry. Consistent with diffuse axonal injury generated by CHIMERA, white matter inflammation, tau immunoreactivity and degeneration were observed in the optic tract and corpus callosum. Finally, pronounced grey matter microgliosis was observed in the olfactory tubercle. Our results provide insight into the mechanisms by which rTBI leads to post-traumatic psychiatric-like symptoms in a novel rat TBI platform.

1. Introduction

Mild traumatic brain injuries (mTBI), including concussions, account for 70–90% of all TBI cases (Frieden et al., 2015). Over 10 million people worldwide and 3 million people in North America sustain a mTBI each year (Hyder et al., 2007). While up to 80% of individuals with mTBI recover spontaneously, a significant number experience enduring symptoms (Schwarzbold et al., 2008), including headaches, mild cognitive dysfunction, emotional lability, psychiatric symptoms, and an increased risk of neurodegenerative disease (Broshek et al., 2015; McKee and Daneshvar, 2015). Highly recurrent concussion such as found in contact sports can be associated with chronic traumatic encephalopathy (CTE), which is defined by the presence of perivascular tau deposits primarily in sulcal depths upon neuropathological

Abbreviations: AUC, area under the curve; BCA, bicinchoninic acid; CCI, controlled cortical impact; CHIMERA, Closed-Head Injury Model of Engineered Rotational Acceleration; CTE, chronic traumatic encephalopathy; DAB, 3,3' Diaminobenzidine; DAPI, 4′,6-diamidino-2-phenylindole; DAT, dopamine transporter; DDT, delay discounting task; GFAP, glial fibrillary acidic protein; i.p., intraperitoneal; IL-1β, interleukin 1β; IL-6, interleukin 6; ITI, intertrial interval; J, joules; LRR, loss of righting reflex; mTBI, mild traumatic brain injury; NF-L, neurofilament-light; NGS, normal goal serum; PBS, phosphate buffered saline; PFA, paraformaldehyde; p-tau, phosphorylated-tau; RIPA, radioimmunoprecipitation assay; RT, room temperature; rTBI, repetitive traumatic brain injury; s.c., sub-cutaneous; TBI, traumatic brain injury; TH, tyrosine hydroxylase; TNF-α, tumor necrosis factor α; VTA, ventral tegmental area

* Corresponding author at: Department of Pathology, Laboratory Medicine, University of British Columbia, 2215 Wesbrook Mall, Vancouver, BC V6T 1Z3, Canada.
E-mail addresses: cole.vonderhaar@mail.wvu.edu (C. Vonder Haar), kris.martens@mail.wvu.edu (K.M. Martens), asma.bashir@ubc.ca (A. Bashir), sophie.stukas@ubc.ca (S. Stukas), cbe37@mail.ubc.ca (C. Barron), cripton@mech.ubc.ca (P.A. Cripton), cwinstanley@psych.ubc.ca (C.A. Winstanley), wcheryl@mail.ubc.ca (C.L. Wellington).

[1] Equal contributions.

https://doi.org/10.1016/j.expneurol.2019.02.012
Received 11 January 2019; Received in revised form 15 February 2019; Accepted 20 February 2019
Available online 26 February 2019

examination (McKee et al., 2016). It is important to recognize that much remains to be learned about the prevalence and clinical course of CTE and about how the clinical sequelae of recurrent concussion may or may not align with the consensus CTE neuropathology (Iverson et al., 2018). Behavioral disinhibition, including increased impulsivity, agitation, and poor executive decision-making is common after TBI (Kim, 2002; Kocka and Gagnon, 2014; Arnould et al., 2016) and can be manifested as substance abuse and aggression (Graham and Cardon, 2008; Bjork et al., 2016; Goswami et al., 2016; Bjork et al., 2017). Importantly, loss of impulse control can also be observed in subjects with rmTBI who are subsequently found to have only mild CTE neuropathology (Mahar et al., 2017; Mez et al., 2017), underscoring the important distinctions between the clinical and neuropathological sequelae of rmTBI.

Choice behavior, and impulsive choice in particular, is strongly regulated by the mesolimbic/mesocortical reward circuit. Dopaminergic neurons in the ventral tegmental area (VTA) project to several brain regions involved in reward processing, including the nucleus accumbens shell (motivation/pleasure), the basolateral amygdala (emotional salience), the orbitofrontal cortex (relative value), the prefrontal cortex (attention/decision), and the hippocampus (memory/context) (Baik, 2013). The mesolimbic circuit facilitates learned associations with motivationally salient events via phasic dopamine release (Brewer and Potenza, 2008). Notably, this is distinct from the nigrostriatal dopaminergic circuit involved in control of motor behavior (Rizzi and Tan, 2017). There is considerable evidence that dopamine physiology is impaired after TBI (Chen et al., 2017). Although relatively few studies have identified aberrant dopaminergic signaling after human TBI (Donnemiller et al., 2000; Wagner et al., 2014; Jenkins et al., 2018), a number of animal studies have established that the dopamine pathway is altered following TBI, reviewed in (Ozga et al., 2018). The dopaminergic system includes long axonal projections from midbrain structures, namely the substantia nigra and VTA, to the striatum and forebrain, respectively (Chen et al., 2017). These projections are easily damaged by shearing forces during rapid acceleration and deceleration, leading to acute hyperdopaminergia followed by chronic hypodopaminergia (Weil and Karelina, 2017) and, in more severe cases, axonal degeneration (Bales et al., 2009; Chen et al., 2017; Merkel et al., 2017). Chronic white matter inflammation that is nearly universal after TBI may also cause sustained alterations in dopamine signaling (Merkel et al., 2017).

Understanding how the psychiatric sequelae of TBI potentially relate to dysfunction of reward pathways will require both in-depth characterization of relevant behaviors and accompanying neuropathology in animal models. Task selection is a particularly critical factor when measuring psychiatric-related dysfunction, as most behavioral assays traditionally used in the preclinical neurotrauma field, such as the Morris Water Maze, Barnes Maze, Elevated Plus Maze, or Rotarod, are relatively simple tasks of spatial memory, anxiety, and motor functions, respectively, which cannot assess the more complex aspects of impulsivity that is highly relevant to human repetitive TBI.

The delay discounting task (DDT) is a well-validated measure of impulsive choice. In this task, the subject chooses between an immediate small reinforcer versus a larger delayed reinforcer. As the delay to the large reinforcer progressively increases across the testing session, subjects tend to switch preference to the smaller reinforcer. Subjects that switch sooner (i.e. can only tolerate small delays) are considered more impulsive. The DDT requires integration of the mesolimbic circuit across the nucleus accumbens shell, basolateral amygdala and orbitofrontal and prefrontal cortices (Winstanley, 2010; Bailey et al., 2016). Importantly, the DDT has high levels of reliability across many species, including humans, with both intra-subject correlations and Cronbach's alpha near 0.9 (Weafer et al., 2013), and can be performed as early as age four in humans (Hodel et al., 2016). Thus, changes to measured levels of impulsivity in experimental animal models have high clinical relevance.

The method by which TBI is induced is an equally important consideration. Some have argued that animals subjected to TBI must present with detectable neuropathology but not necessarily demonstrate behavioral deficits, while others have suggested that the opposite may be more representative of the human condition, particularly for mTBI. This debate has led to the development of a wide variety of methods to induce experimental mTBI in animals and an equally diverse repertoire of methods by which such models are assessed. The Closed-Head Impact Model of Engineered Rotational Acceleration (CHIMERA) model of mTBI (Namjoshi et al., 2014, 2017) is a non-surgical impact acceleration model that delivers precise mechanical inputs to reliably induce a combination of linear and rotational movement in a freely-moving head to produce mTBI (Namjoshi et al., 2014). Robust pathological alterations associated with CHIMERA include diffuse axonal damage across multiple white matter tracts, and microglial and astrocyte reactivity as a function of impact energy (Namjoshi et al., 2014, 2017). As a non-surgical method, CHIMERA is ideal to model the effects of multiple mTBIs. However, behavioral assessments in mice are somewhat limited to the relatively simple tasks of motor, memory and anxiety that mice can readily be trained on.

Compared to mice, rats are far more suitable for the study of complex behaviors, including sensitive operant behaviors that measure chronic deficits that can persist for months after surgical TBI induced by the most historical model called open-head controlled cortical impact (CCI) (Vonder Haar et al., 2016, 2017). As this traditional version of CCI is not suitable to investigate repetitive TBI, we therefore adapted the CHIMERA system to rats to enable use of the DDT to explore the relationship between repetitive TBI, impulsive choice, white matter pathology, and dopaminergic signaling. We accomplished this by training rats to perform the DDT, and then subjected them to five consecutive CHIMERA injuries or sham procedures spaced two weeks apart. At end-point, we performed histological and biochemical analyses to elucidate the complex interrelationship between rTBI and impulsivity, allowing mechanisms and potential targets for intervention to be identified.

2. Materials and methods

2.1. Study aim

The overall aim of this study was to investigate the relationships between impulsive choice and neuropathology in rats subjected to 5 consecutive CHIMERA impacts at 2.9J (first impact) and 2.4J (subsequent impacts) with a 14d inter-injury interval. These parameters were selected, in part, empirically, to balance the ethical use of animals for the behavioral and neuropathological objectives. As assessment of impulsive choice using the DDT requires extensive testing, we selected the 14d interval to allow collection of DDT data for 10 sessions (5 sessions/week) after each injury. We terminated the study after 5 successive TBIs as robust behavioral differences were observed and neuropathological assessment was warranted. For the neuropathological arm of the study, we aimed to identify differences between sham and TBI groups that could explain their different behaviors, as well as to determine whether rat CHIMERA produces diffuse axonal injury similar to mouse CHIMERA.

2.2. Animals

Subjects were thirty-five male Long-Evans rats (Charles River, Wilmington, MA). Subjects were approximately 3 months of age at the start of training, 4.5 months at the first injury, and 6 months at euthanasia. Rats were food restricted to 85% of free-feeding weight (14–16 g PicoLab Rodent Diet 20 (62.4% carbohydrate, 24.5% protein, 13.1% fat) daily); water was available ad libitum. Rats were triple-housed throughout the duration of the study in trapezoidal Optirat cages (356 × 485 × 218 cm, Animal Care Systems, Centennial, CO) on

a reverse light cycle (12 h:12 h) with a plastic hut and shredded paper towel available as enrichment. All procedures were approved by the University of British Columbia Animal Care Committee (A15-0040) and compliant with guidelines from the Canadian Council on Animal Care.

2.3. Apparatus

Training and testing took place in a bank of twelve standard five-hole operant chambers with a stimulus light at the back of each hole, and an infrared beam to measure nose pokes (Med Associates, St. Albans, VT). On the other side were two retractable levers with lights above, a house-light, and a food tray with a sucrose pellet dispenser attached (45 mg pellets, Bio-Serv, Flemington, NJ). Chambers were controlled by custom software written in Med-PC IV.

2.4. Behavioral training

Initial Training: Training on the delay discounting task (DDT) was performed as outlined previously (Vonder Haar et al., 2017). The left, center, and right (1, 3, 5) holes in the five-choice panel and the pellet dispenser were used in this study. Briefly, rats were habituated to the chamber with sugar pellets placed in the food hopper, and in holes 1, 3, and 5 for one to two sessions. In the first stage of training, rats learned to respond to an illuminated hole 3 to receive one pellet until they successfully completed 30 trials in a single session. In stage two of training, rats responded first to illumination of hole 3, which turned on a light in either hole 1 or 5 (pseudo-randomly) and correct responses were reinforced with a single sugar pellet. Finally, in the last stage, a differential was introduced, with hole 1 delivering four sugar pellets and hole 5 delivering a single pellet. The location of the larger reinforcer hole (hole 1 or 5) was kept constant for each rat throughout training and testing, but was counterbalanced between subjects.

Delay Discounting Task: After the above training, the DDT began. Sessions lasted forty minutes and consisted of four blocks of twelve trials with a fixed 40 s intertrial interval (ITI). A trial began with the illumination of hole 3, and a nose poke would illuminate both choice holes 1 and 5. Failure to respond within 10 s was scored as an omission and activated the ITI. Rats chose between the large (four pellets) and small (one pellet) option, counterbalanced as above. The small option was always delivered immediately, while the delay to the large option increased in a step-wise fashion across successive blocks of trials, from 0 to 5, 10, and finally 20 s. Every block began with two forced-choice trials to ensure rats were exposed to the current delay contingency. After a choice was made and the reinforcer delivered, there was an ITI equal to the remaining trial time (40 s minus the delay to reinforcement). Rats were tested until a statistically stable choice baseline emerged, which required approximately thirty sessions. A total of N = 35 rats successfully learned the DDT were matched for baseline performance and randomly assigned to sham (N = 11) or CHIMERA TBI (N = 24) groups. Testing resumed 24 h after each subsequent injury and continued for two weeks (ten sessions at five sessions/week) until the next injury. A total of 5 cycles of injury and recovery were performed in this study.

2.5. Rat CHIMERA TBI procedure

Meloxicam (5 mg/kg, subcutaneously [s.c.]; Boehringer Ingelheim Vetmedica Inc., Missouri) was administered 1 h prior to injury for analgesia. Rats were anesthetized with 5% isoflurane and placed supine on the rat CHIMERA device. A nose cone delivered 2% isoflurane while rats were strapped to the device with one Velcro strap around the abdomen that was fastened firmly to secure the animal, and another around the thorax that was loosely fastened to prevent hyperflexion of the thoracic spine in the sagittal plane during impact. Once secured, rats received a lactated ringer solution (5 mL, s.c.). Head position was verified as centered on the impact point approximately in front of bregma. The first injury was delivered at 7.6 m/s (2.9 J), but was subsequently reduced to 6.9 m/s (2.4J) for injuries 2–5 due to mortality of 4 rats during the first CHIMERA session (see Results). Piston velocities were obtained using photogate sensors on the rat CHIMERA device. Immediately after impact, animals were placed in a heated recovery cage and the time to right was recorded. Total procedure time, including anesthetic induction, took approximately 3 min. Sham animals received anesthesia yoked to the duration of injured animals, analgesic, hydration, and positioning on the CHIMERA device, but no impact.

2.6. Euthanasia and tissue collection

Rats were euthanized at the conclusion of the final testing period, eleven weeks after initial injury and three weeks after the fifth and final injury. Briefly, rats were anesthetized with a combination of ketamine (100 mg/kg, intraperitoneal [i.p.]; Zoetis, New Jersey) and xylazine (7 mg/kg, i.p.; Bayer, Pennsylvania) and transcardially perfused with ice-cold heparinized phosphate-buffered saline (PBS). Brains were rapidly removed and one hemisphere was post-fixed in a 4% paraformaldehyde (PFA) solution for histology, while the other was sectioned into forebrain (7.56 to ~0 mm from bregma), midbrain (~0 to −3 mm from bregma) and hindbrain with a razor blade and immediately frozen on dry ice for biochemistry.

2.7. Immunohistochemical procedures

Hemibrains were post-fixed in 4% PFA for 2 d, then cryoprotected with 30% sucrose in PBS and 0.01% sodium azide for 3-4 d, after which 40 μm-thick coronal sections were cut using a cryotome (Leica Biosystems, Concord, ON). Immunohistochemistry was performed largely as described (Namjoshi et al., 2013) and included staining for tyrosine hydroxylase (TH) and dopamine active transporter (DAT) to detect dopaminergic neurons, Iba-1 to detect microglia, glial fibrillary acidic protein (GFAP) to detect astrocytes, SMI312 to detect neurofilament-light, CP13 to detect S202 phosphorylated tau, and silver staining to detect degenerating, argyrophilic axons. Sections stained for dopaminergic neurons (TH, DAT) followed an immunofluorescent protocol. Briefly, sections were washed in PBS and 0.5% Tween-20 for permeabilization, then blocked with 5% normal goat serum (NGS; Millipore Sigma S26-100ML) for 1 h at room temperature (RT). Sections were incubated with primary antibodies for TH and DAT overnight at 4 °C. Sections were then incubated with Alexa-Fluor secondary antibodies (Invitrogen, 1:1000) for visualization using fluorescence microscopy. For nuclear co-stain, mounted sections were coverslipped with ProLong Gold Antifade Mountant with 4′,6-diamidino-2-phenylindole (DAPI) (Invitrogen P36935). Sections stained for Fluoro Jade-C were co-stained with TH for degenerating dopaminergic neurons. Sections were washed in PBS and 0.5% Tween-20 for permeabilization, then blocked with 5% NGS for 1 h at RT. Sections were incubated with primary antibody for TH overnight at 4 °C. Sections were then incubated with Alexa-Fluor 594 secondary for 4 h at RT. After washing, sectioned were mounted on charged slides and dried. An abridged Fluoro-Jade protocol was utilized to preserve the fluorescent TH signal. Slides were immersed on basic ethanol for 4 min, followed by a 2-min rinse in 70% ethanol, then 1-min rinse in distilled water. Slides were incubated in 0.06% potassium permanganate for 2 min, rinsed in distilled water for 1 min, then incubated in 0.0001% FluoroJade in 0.01% acetic acid for 10 min. After washes and drying, sections were coverslipped with ProLong Gold Antifade Mountant with DAPI.

Sections stained for Iba-1, CP-13, NFL and GFAP followed a 3,3′ Diaminobenzidine (DAB) staining protocol. Briefly, sections were quenched with hydrogen peroxide for 10 min and blocked with 5% NGS or 5% skim milk in PBS for 1 h at RT. Sections were incubated with primary antibodies overnight at 4 °C. Sections were then incubated with biotin-conjugated secondary antibodies (1:1000) and detected using a

colorimetric procedure by incubating with ABC reagent (Vector Labs PK-6100, 1:400) before colour development with DAB (Sigma D5637-1G).

Antibodies and dilutions were: TH (Millipore 657,012, 1:500), DAT (Millipore MAB369, 1:500), Iba-1 (Wako 019-19741, 1:1000), CP-13 (Gift from Peter Davies, 1:500), NF-L (Abcam SMI-312 1:1000), and GFAP (Abcam ab7260, 1:500). Axonal injury was histologically evaluated by Neurosilver staining (FD Neurotechnologies) following the manufacturer's instructions as described (Namjoshi et al., 2013).

2.8. Brain imaging and staining quantification

Entire coronal sections were imaged using a Zeiss AxioScan Z1 slide scanner at 20× magnification. DAT and TH images of the VTA, basolateral amygdala, nucleus accumbens shell, olfactory tubercle, and orbitofrontal cortex were acquired as 0.5 μm z-stacks with a 40× oil objective on a Zeiss confocal laser scanning microscope (LSM880). FluoroJade-C and TH images of the VTA and olfactory tubercle were acquired as 1 μm z-stacks at 20× a Zeiss confocal laser scanning microscope. Images were flattened using the max projection function of Zen Black Pro software (v.14.0.12.201). Excitation and acquisition parameters were constrained across all images. The anterior commissure size and position relative to the corpus callosum and dorsal/anterior hippocampus were used as anatomical landmarks for consistent coronal section selection. Image quantification was performed using Image J (NIH), unless otherwise specified, on sections from N = 7–10 rats in the Sham group and N = 12–16 from the 5x TBI group.

For TH and DAT quantification, images were manually thresholded and binarized. For puncta count and colocalization, binarized images were masked and analyzed using CellProfiler cell image analysis software (http://www.cellprofiler.org). Puncta size was set between 1 and 50 pixel units. A quantitative average of two acquired images per ROI was calculated and statistical analyses were performed on averaged values. CellProfiler pipelines can be made available upon request. For FluoroJade-C quantification, an ImageJ macro script was written to binarize, threshold, and convert the images to masks. To measure the colocalization of FluoroJade to TH-positive signal, the FluoroJade signal was measured within the TH mask and reported as percent colocalization. Total FluoroJade signal, expressed as a percentage of the region, was also reported. For Iba-1 and GFAP quantification in grey and white matter regions, ROIs were manually isolated and thresholded; subsequently, count per area was used to determine differences between sham and 5xTBI groups after filtering background noise of particles < 250 pixel units. For NF-L quantification, images were manually isolated, converted to 8 bit and thresholded using the ImageJ Auto-Thresholding function “Max Entropy”. Background noise of particle size < 17μm^2 or with circularity < 0.2 were filtered. The number of axonal swellings per area of optic tract was then reported. For CP13 quantification, white matter areas, including corpus callosum and optic tract, were cropped and converted to 8 bit and thresholded. Background noise of particle size < 3.5μm^2 were filtered. The number of stained particles per area of the white matter area was then reported. For grey matter areas, including prefrontal cortex (prelimbic and infralimbic area), layer 2–5 was aligned and cropped. Quantification was not possible due to strong variations in background stain intensity. However, CP13-positive neurons were manually identified based on shape (neuronal cell body and neurite). Representative images of the injury group were then reported. Silver staining images were quantified by manually isolating ROIs, thresholding and reporting the percentage area containing signal relative to the white matter area, as described (Namjoshi et al., 2013).

2.9. Biochemical preparation and analysis of inflammatory cytokines, tau, and NF-L

Midbrain and forebrain sections were homogenized in 8-volumes of ice-cold radioimmunoprecipitation assay (RIPA) lysis buffer containing protease and phosphatase inhibitor cocktails (Roche, Branford, CT) and centrifuged at 9000 rpm for 10 min at 4 °C. The supernatant was extracted and frozen at −80 °C until analyzed. Total protein concentration was measured by bicinchoninic acid (BCA) assay (Biorad, Redmond, WA). Forebrain and midbrain regions were analyzed separately given the frontal-sensitive nature of impulsivity (Clark et al., 2004; Winstanley, 2007). Forebrain and midbrain homogenates were diluted 1:2 in dilution buffer provided in the assay kit, and incubated overnight (4 °C) in a multiplex ELISA to measure IL-1β, IL-6, and TNF-α (V-plex K15059D, Mesoscale Diagnostics). Samples were read on a microplate reader (Mesoscale Sector Imager). For analysis of total and phosphorylated tau (threonine 231), brain homogenates were diluted 1:50 in 10% blocker A in the provided Tris wash buffer, and assayed for tau and phosphorylated tau (p-tau; thr231) levels in a duplex ELISA (Mesoscale Diagnostics, K15121D), following the manufacturer's protocol. All analyte concentrations were normalized to the total protein concentration in the lysate.

2.10. Data analysis and statistics

In previous work, we used the fit of a hyberbolic discounting function to analyze choice behavior (Vonder Haar et al., 2017). This formula works best when multiple data points are available (e.g. one week of data). In the current study, this was not feasible because a measure of daily change as a result of the injury was a planned part of the study. We therefore elected to use the measure of Area Under the Curve (AUC) (Myerson et al., 2001), which is calculated by drawing straight lines between data points and calculating the percent or proportion of total area that falls beneath those lines. This measure correlates with the fitted discounting function and allows for more reliable daily measurement of choice. Curve fits (using the hyperbolic function) for an entire week of data are still provided alongside the raw data for context.

Statistical tests for behavioral and biochemical outcomes were conducted using R statistical software (http://www.r-project.org/), using the *stats*, *lme4* and *lmerTest* libraries. Repeated measures data (delay discounting, loss of righting, impulsive choice impairment status) were analyzed using mixed effects regression, with individual rat intercepts as the random effect. Linear regressions were used for group comparisons, while piecewise regression (on AUC) and logistic mixed effects regression (on impairment status) evaluated within-subjects effects. P-values were estimated using the *lmerTest* library. Cytokine and tau protein levels were compared in one-way ANOVAs. Any main effects of group were followed by a Dunnett's post-hoc test to compare to the sham group. Statistical analyses for histological quantification were conducted on GraphPad Prism (v6.07). Unless otherwise specified, Welch's t-test was utilized as the groups were normally distributed, but had unequal variances and unequal sample sizes. Ratio data was log transformed to improve normality assumptions. Two-tailed parametric Pearson coefficients with a 95% confidence interval were utilized where r values were calculated for X vs every Y in the data set. For all statistical tests, a p-value of < 0.05 was considered significant.

3. Results

3.1. Rat CHIMERA design

A new CHIMERA device was engineered to produce TBI in rats (Fig. 1A–C). To produce the desired impact characteristics, a 100 g stainless-steel piston body with a diameter of 0.75 and a 0.394 (10 mm)

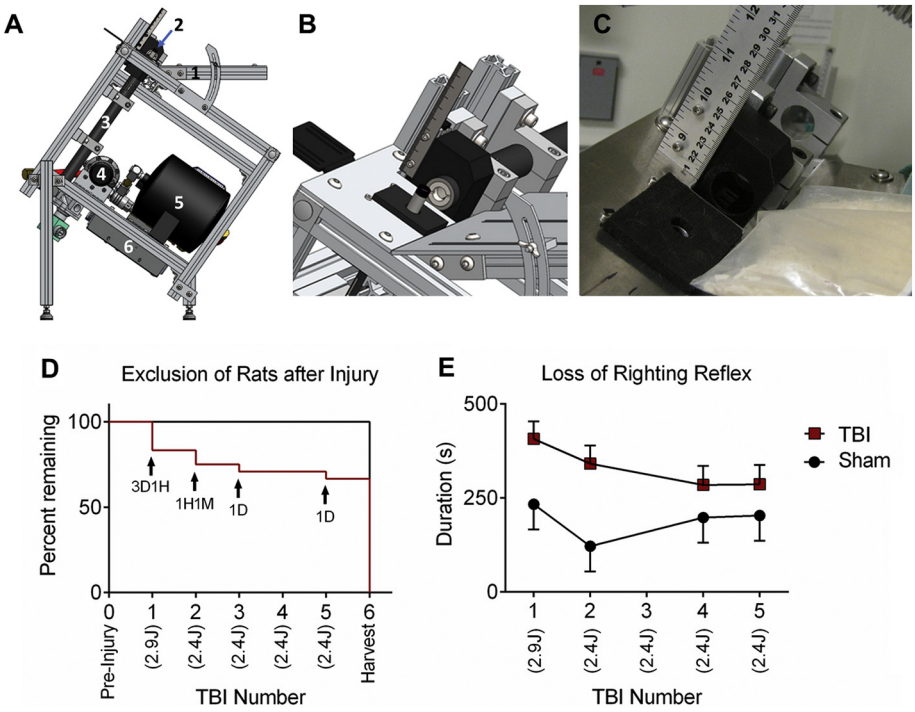

Fig. 1. Schematics of the rat Closed-Head Impact Model of Engineered Rotational Acceleration (CHIMERA), mortality rates and loss of righting reflex latency following CHIMERA TBI. (A) Rat CHIMERA digital schematic is shown from frontal view. Parts are labelled with numbers as follows: 1) body plate, 2) impact piston, 3) vertical-impact piston barrel, 4) air pressure regulator, 5) air tank, 6) CHIMERA motherboard. (B) Zoomed in head plate shown for clarity. (C) Photo of rat CHIMERA animal platform. (D) Cumulative exposure to TBI at 2.9J (1st week) or 2.4J (2nd to 5th week) resulted in a final exclusion rate of 33%. The abbreviations under the exclusion curve indicate the number of animals excluded after each TBI. D: pre-mature death, H: humane endpoint, M: morbidity, including blindness. (E) Repetitive CHIMERA TBI in resulted in an increase that trended towards significance for the duration of loss of righting reflex (LRR) (p = .057). LRR at week 3 was not recorded due to computer failure.

tip was made. It was also necessary to increase the impact energy (piston velocity) substantially to obtain the desired head kinematics. Larger air pressures were required to provide the necessary impact energies, which required using higher capacity pneumatic components specifically for the pressure regulator and pressure gauge. With higher impact energies, additional venting was also required to prevent the piston from rebounding off of the compressed air and striking the head a second time. Venting was accomplished by installing a second solenoid valve with a pipe tee at the bottom of the barrel that would open after the piston had finished accelerating.

To accommodate the larger size of the rat, the length of the body platform was increased from 6 to 9 in. Animal body restraints were adjusted by using a rice-filled bag instead of a carved closed cell foam bed, and by adapting the locations of the Velcro straps. The head plate was modified to accommodate the larger impactor tip and to align the head properly with the impact location. A 30° body-plate inclination angle allowed the frontal and parietal bones to lie flat over the hole in the head plate. To prevent rats from sliding down the body platform at this angle, the device frame was inclined to match the angle of the body platform such that the body was horizontal and the head was inclined relative to the ground.

In addition to these structural changes, the rat CHIMERA device also included the first implementation of an electronic controller. This controller offers two major functional improvements: direct measurement of piston impact velocity and improved impact energy repeatability. The controller utilizes a pair of infrared photo-interrupters located at the end of the piston barrel (nearest the head), which send a signal to the controller when the piston passes by each of them. With a constant distance between the photo-interrupter pair, the piston velocity can be determined by dividing this distance by the time between the signals. Photogate velocity readings are calibrated using velocity measurements obtained from analysis of high-speed video of the piston tip as it protrudes beyond the head plate.

3.2. Injury-related morbidity/mortality

The total number of animals that were removed over the course of the study due to death, humane endpoint, or morbidity was eight of twenty-four injured animals (33%) and 0 of 11 sham animals (0%) (Fig. 1D). During first injury at 7.5 m/s (2.9 J), three of twenty-four rats in the CHIMERA TBI group died and one reached humane endpoint and required euthanasia during acute recovery. Specifically, two animals died as a result of intracranial hemorrhage, one died as a result of nasal hemorrhage, and one was humanely euthanized after poor recovery and showed signs of intracranial hemorrhage on necropsy, leaving N = 20 rats in the CHIMERA TBI group that progressed to injury 2. Upon consultation with our veterinary staff, we reduced injury severity to 6.9 m/s (2.4 J) for subsequent injuries to limit mortality. The recorded average impact velocity for injury 1 was 7.56 m/s (2.86 J energy), while injuries 2–5 averaged 6.95 m/s (2.42 J energy). After injury 2, one rat was humanely euthanized after poor recovery and showed intracranial hemorrhage on necropsy, one was removed from the study due to blindness, and one displayed transient seizure activity but recovered, leaving N = 18 rats in the CHIMERA TBI group that progressed to injury 3. After injury 3, one rat displayed seizures and died due to intracranial hemorrhage, leaving N = 17 rats in the TBI group that progressed to injury 4. There was no morbidity or mortality for injury 4, and one rat died after injury 5, leaving a total of N = 16 rats that completed the CHIMERA TBI arm of the study. No morbidity or mortality was observed for the N = 11 rats in sham group and all sham animals completed the study. Because mixed-effects regression does not require list-wise deletion (i.e., removal of a rat's data from the study), all available data were used, even for rats with early mortality. The only behavioral exclusion was the rat that developed blindness. Histological analyses only included data from rats that completed the study as it was not feasible to collect tissue in the cases of early mortality.

3.3. Loss of righting reflex latency

Loss of righting reflex (LRR) was recorded for all animals (Fig. 1E), however, data from injury 3 was lost due to a computer malfunction. To control for anesthesia effects, the anesthesia time for each sham procedure was yoked to an injured animal. A mixed effects linear regression (LRR~Group*Injury#) revealed that CHIMERA injury tended to increase LRR duration that approached but did not reach statistical significance across the entire study (β = 0.69, t = 2.06, p = .057),

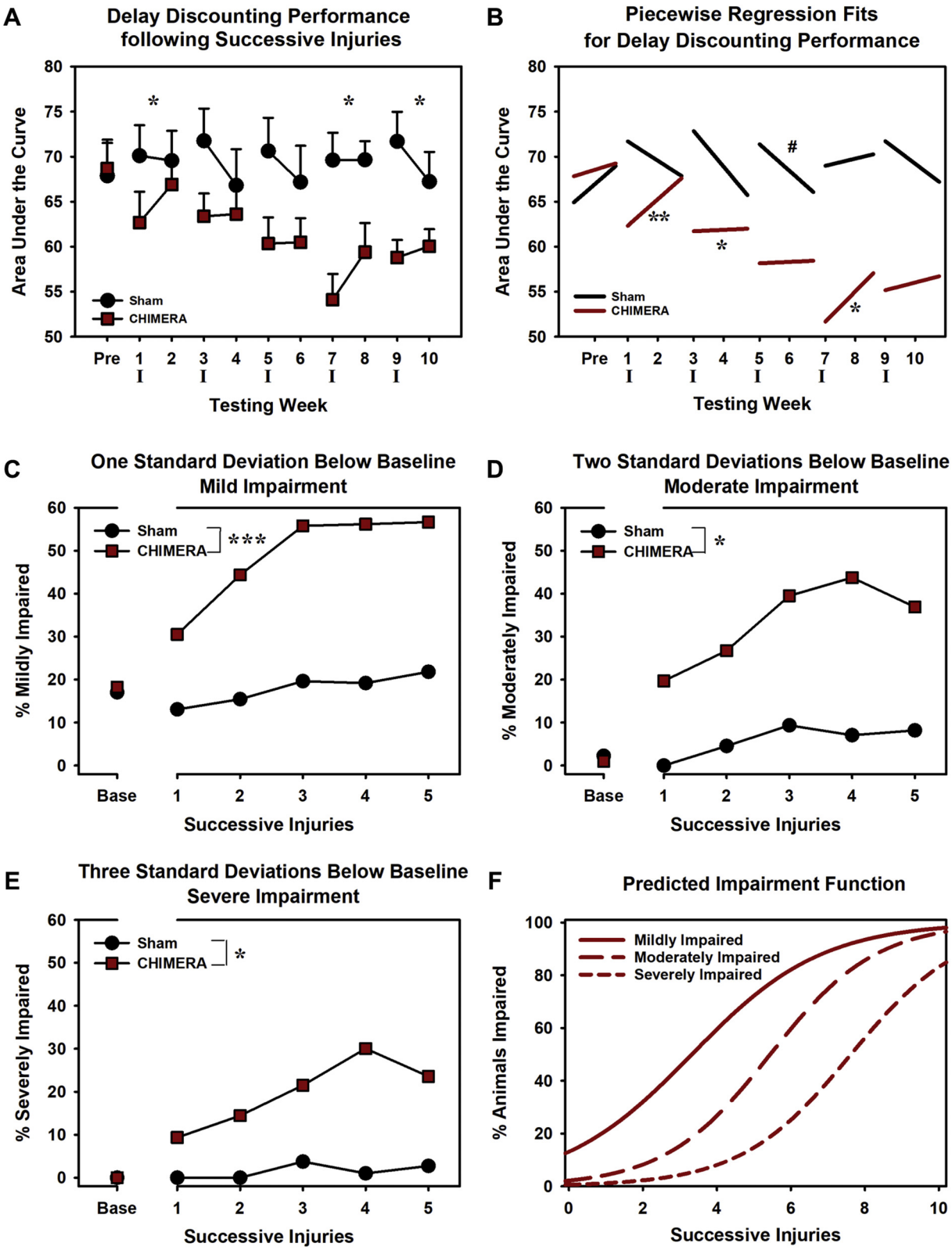

Fig. 2. Impulsive decision-making increases as a function of CHIMERA injury exposure. (A) Averaged area under the curve (AUC) for each group across time (mean + SEM); smaller AUC values are representative of increased impulsivity. Overall, there was a significant effect of group on impulsivity ($p = .041$). Individual analyses revealed that CHIMERA animals were significantly different from sham after the first (Group X Session interaction: $p = .013$), fourth, and fifth injuries (main effect of Group: p's < 0.016). (B) Piecewise regression fits to compare the effects of each injury within subjects. Sham animals significantly improved impulsivity from injury 2 to injury 3 ($p = .039$). CHIMERA animals got significantly worse after injuries, 1, 2, and 4 (p's < 0.024). (C) Mild impairment, defined as one standard deviation below individual baseline increased over time in the CHIMERA group ($p < .001$). (D) Moderate impairment also increased across time for CHIMERA animals ($p = .047$). (E) Severe impairment levels were significantly increased overall in the CHIMERA group ($p = .029$). (F) Prediction function showing that the likelihood of impairment increases as a function of successive injuries for CHIMERA animals. Symbols: * = $p < .05$; ** = $p < .01$; *** = $p < .001$ relative to sham. # = $p < .05$ for Sham animals. Data are means ± SEM for (A), regression predictions for (B,F), and means for (C-E).

likely driven by considerable LRR durations in injuries 1 and 2 for CHIMERA rats (Fig. 1E). LRR duration tended to decrease across subsequent CHIMERA injuries, however this decrease did not reach significance.

3.4. Impulsive decision-making increases as a function of CHIMERA injury exposure

CHIMERA TBI and sham groups were evaluated for impulsivity on the DDT by measuring their area under the discounting curve (AUC) followed by linear mixed effects regression analysis (AUC~Group*Injury #). Raw data and curve fitting using a hyperbolic function for an entire week of data are provided for context (Fig. S1A, S1B). As the interaction of Group and Injury number was significant ($p < .001$), follow-up linear mixed effects regression analyses were performed for the ten sessions after each injury (AUC~Group*Session). The CHIMERA TBI group displayed significantly increased impulsivity (reduced AUC) after injuries 4 and 5 (p's < 0.016, Fig. 2A). However, a significant Group x Session interaction on Injury 1 ($p = .013$), showed a significant, but transient decline in performance, and the interaction on Injury 2 also approached significance ($p = .087$; Fig. 2A; summarized in Table 1).

The lack of early group differences can largely be attributed to considerable heterogeneity in individual rats' responses to injuries. To examine the effects of injury within subjects, a piecewise linear mixed effects regression was then performed on impulsivity as a function of injury number and post-injury slope (AUC~Injury1 + Injury1 Slope … + Injury5 + Injury5 Slope + Overall Time) separately for each group (Fig. 2B). Sham animals displayed one significant *decrease* in impulsive decision-making from injury 2 to injury 3 ($p = .039$). By contrast, the CHIMERA TBI group showed significant increases in impulsivity from baseline to Injury 1 ($p = .006$), from Injury 1 to Injury 2 ($p = .023$), and from Injury 3 to Injury 4 ($p = .010$; see Table 2 for a summary of statistics), suggesting that substantial effects still occur at earlier injuries.

An additional means of considering the cumulative effects of injury is to determine the likelihood of impairment as a result of successive TBIs. To analyze this, we performed linear mixed effects logistic regression on the percent of animals that showed mild, moderate, or severe impairments in impulsive decision-making (defined as > 1, 2, or 3 standard deviations below their own individual baseline; Impaired~Group*Injury#) (Fig. 2C–E). A 1 standard deviation increase in impulsivity occurs in slightly under 20% of sessions (baseline), whereas a 2 standard deviation or greater change occurs extremely rarely under uninjured conditions. Successive CHIMERA injuries produced a significant shift in the percent of animals displaying > 1 or 2 standard deviations in impairment (1 SD: $b = 0.44, z = 4.87, p < .001$; 2 SD: $b = 0.29$, $z = 1.98$, $p = .047$). When measured at 3 standard deviations, there was no interaction, but main effects of group and cumulative injuries remained (Group: $b = 3.72$, $z = 2.19$, $p = .029$; Injury: $b = 0.60$, $z = 2.13$, $p = .033$;). Because injured animals were significantly different from sham when measured at 1, 2, or 3 standard deviations below baseline, a separate logistic function was calculated with only injured animals (Impaired~Injury) to evaluate the predicted impairment functions as a result of successive injuries (Fig. 2F). Extrapolated from these data, the ED50 for mild impairment is 3.32 CHIMERA injuries, for moderate impairment is 5.44 CHIMERA injuries, and for severe impairment is 7.62 CHIMERA injuries (Fig. 2F).

3.5. 5xTBI induces neuropathological changes consistent with disruption of the mesolimbic reward circuit

The robust alteration of impulsive choice prompted us to test for neuropathological changes in the mesolimbic reward pathway. Intriguingly, quantitation of tyrosine hydroxylase (TH)-positive puncta showed that the reduction of dopaminergic innervation trended towards significance in the olfactory tubercle in the 5xTBI group ($p = .0545$), with no significant changes compared to sham animals in the VTA, basolateral amygdala, nucleus accumbens (shell) or orbitofrontal cortex (Fig. S2A). As it is important to assess the synaptic lifetime of dopamine through probing of its reuptake machinery, we also quantified dopamine transporter (DAT) in the aforementioned regions and observed no significant changes (Fig. S2B). However, when DAT:TH colocalization were assessed, we found that colocalization within the olfactory tubercle was significantly reduced ($p = .0308$), whereas the VTA, basolateral amygdala, nucleus accumbens (shell) and orbitofrontal cortex showed no differences following repetitive injury (Fig. 3B–E). Analysis of the nigrostriatal dopaminergic pathway showed that 5xTBI has no significant effect on TH, DAT or their colocalization within the substantia nigra and dorsolateral striatum (Fig. S3A–C). These observations support a selective effect of repetitive CHIMERA TBI on the dopaminergic mesolimbic reward pathway consistent with our behavioral observations of increased impulsivity without alterations in overall motor behavior. As the olfactory tubercle is located almost exactly opposite to the injury site, and may be vulnerable to contrecoup injury, we postulated that the region might be undergoing neuronal degeneration. However, quantification of FluoroJade-C signal colocalized with TH-positive neurons and puncta showed no significant changes in the VTA and olfactory tubercle following 5xTBI (Fig. S4A). Furthermore, no significant differences in total FluoroJade signal, expressed as a percentage of the entire region of interest, were observed in the ventral tegmental area and the olfactory tubercle (Fig. S4B).

3.6. 5xTBI induces white matter inflammation and degeneration

We investigated injury-related inflammatory and degenerative changes in two white matter tracts sensitive to murine CHIMERA injury, namely the corpus callosum and optic tract, using silver staining, and immunohistochemistry for microglia (Iba-1), glial fibrillary acidic protein (GFAP), neurofilament-light (NF-L) and phosphorylated (p-) tau (Fig. 4A–G, Fig. 5A–G). In the corpus callosum, no changes were observed by silver staining (Fig. 4C), however a significant increase in Iba-1 and GFAP immunoreactivity was evident (Fig. 4D, Iba-1: $p = .0080$; Fig. 4E, GFAP: $p = .0007$), indicating increases in microglial and astrocytic recruitment and/or proliferation. While there were no changes in NF-L immunoreactivity following 5xTBI, we saw an interesting decrease in corpus callosum thickness (Fig. 4G, $p = .0248$). Within the optic tract, we observed significant increases in silver staining (Fig. 5C; $p < .0001$) and Iba-1 immunoreactivity (Fig. 5D; $p < .0001$). However, we did not see changes in GFAP and NF-L immunoreactivity in the optic tract (Fig. 5E, F). We also observed increased p-tau within the optic tract following 5xTBI associated with distinct dystrophic axonal punctae (Fig. 5G; $p < .0001$).

3.7. 5xTBI induces selective changes in p-tau and microglia within the mesolimbic pathway

We examined grey matter regions involved in the mesolimbic pathway for the presence of pre-tangle-like aggregates and dystrophic neurites using p-tau immunohistochemistry. Increased p-tau S202 was qualitatively observed within the nucleus accumbens (shell) and orbitofrontal cortex, but not in the VTA, basolateral amygdala and olfactory tubercle (Fig. 6A, B). Quantification was not possible due to strong individual variations in background stain intensity. Upon examination of the mesolimbic pathway using Iba-1 immunohistochemistry (Fig. 7A, B), we saw increased Iba-1 within the olfactory tubercle, but not in the VTA, basolateral amygdala, nucleus accumbens (shell), or orbitofrontal cortex (Fig. 7C–G). This inflammatory profile may be related to decreased dopaminergic innervation into the olfactory tubercle.

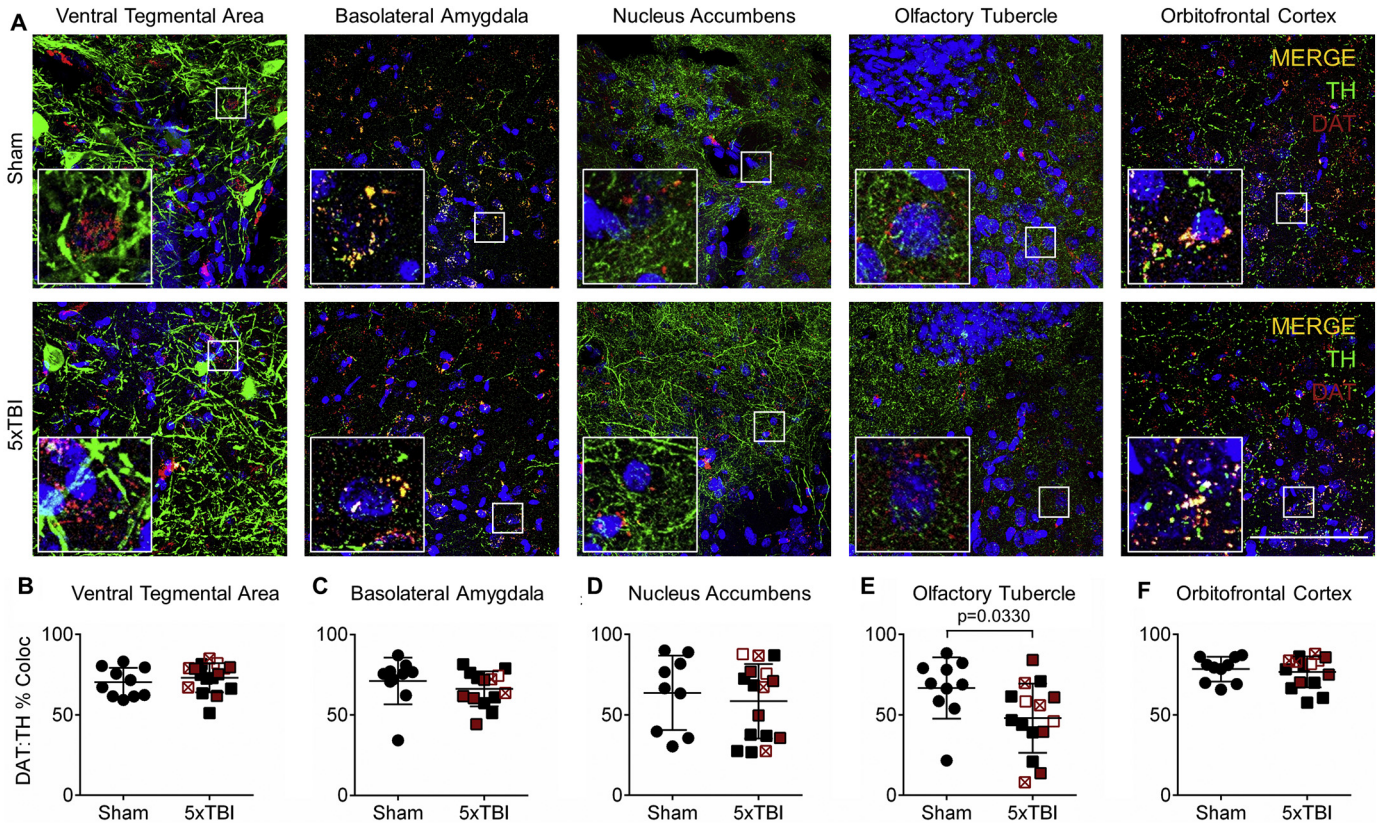

Fig. 3. 5xTBI induces neuropathological changes consistent with disruption of the mesolimbic reward circuit. (A) A panel displaying 40× TH and DAT images within the mesolimbic system with high magnification insets; scale bar = 100 μm. (B) After 5xTBI, no differences in DAT to TH colocalization were observed in the ventral tegmental area, (C) basolateral amygdala, and (D) nucleus accumbens shell. Interestingly, there was a significant decrease in DAT:TH colocalization within the (E) olfactory tubercle of the ventral striatum ($p = .0330$), due to a trending decrease in the presence of TH+ neurons. (F) No differences were observed in the orbitofrontal cortex. In (B–F), TBI samples are colour coded based on performance on the delay discounting task relative to individual baseline: solid black = within baseline; red border, white fill = 1 SD below baseline; red cross = 2 SD below baseline; solid red = 3 SD below baseline. Data are presented as mean ± SD. (For interpretation of the references to colour in this figure legend, the reader is referred to the web version of this article.)

3.8. Correlations between DDT performance and neuropathology

We calculated Pearson correlations using sham and 5xTBI data extracted from final performance on DDT performance with the neuropathological observations of p-tau deposition and corpus callosum thinning. We observed a significant negative correlation between degree of impairment and quantified p-tau in the optic tract ($r = -0.5496$, $p = .0036$; Fig. 8A). Conversely, corpus callosum thickness was positively correlated with lesser impairments, suggesting that subjects with callosal thinning exhibited increased impulsivity ($r = 0.4647$, $p = .0450$; Fig. 8B). We also assessed correlations between DDT performance and all significant neuropathological outcomes, presented in Table 4. None of the other significant neuropathological findings were found to correlate with DDT performance.

3.9. No significant changes in tau or inflammatory biochemical markers in fore- or midbrain homogenates are observed after 5X TBI

ELISA was used to test for altered biochemical profiles of total tau, p-tau, IL-1β, Il-6 and TNF-α in forebrain and midbrain segments at endpoint. No significant differences were observed for any analyte tested, nor of the p-tau:t-tau ratio, between sham and 5xTBI groups for either forebrain or midbrain segments (Table 3), highlighting the importance of the regional specificity shown above.

4. Discussion

A variety of neurological problems and increased risk for psychiatric disease are associated with both single and repetitive TBI (Donnell et al., 2012; Wilk et al., 2012; Broshek et al., 2015). The current study was designed to explore the relationship between repetitive TBI, impulsive choice, white matter pathology and dopaminergic signaling in rats. We adapted CHIMERA, an established model of diffuse axonal injury in mice, to rats, and demonstrated that repeated TBIs caused progressively increased impulsive choice, reduced dopaminergic terminals in the olfactory tubercle of the ventral striatum, and caused robust white matter pathology including neuroinflammation, tau pathology and atrophy. Thus, repetitive rat CHIMERA produces a constellation of behavioral and neuropathological outcomes and may serve as useful model to investigate the sequelae of rTBI. Impulsivity, broadly defined as action without forethought (Winstanley et al., 2006), is a relatively common psychiatric-like complication as a result of moderate-to-severe TBI (Bjork et al., 2016; Goswami et al., 2016). Choice impulsivity, or decisions that result in short-term gains to the detriment of long-term outcomes, is specifically increased following severe, focal TBI (Dixon et al., 2005; Rochat et al., 2010). Reports of specific impulsivity measurements following human concussion are somewhat limited; however, many studies indicate that impulsive phenotypes or impulsive-related disorders are associated with mild brain injury (Graham and Cardon, 2008; Bjork et al., 2016; Goswami et al., 2016). Studies in athletes may provide a better quantification of mTBI incidence, and indeed, such research demonstrates a relationship between items such as total fight exposure (in boxers and mixed martial arts fighters), reduced subcortical structure volume, and trait impulsivity as measured by questionnaires (Banks et al., 2014).

The underlying etiology of impulsivity and other psychiatric-like

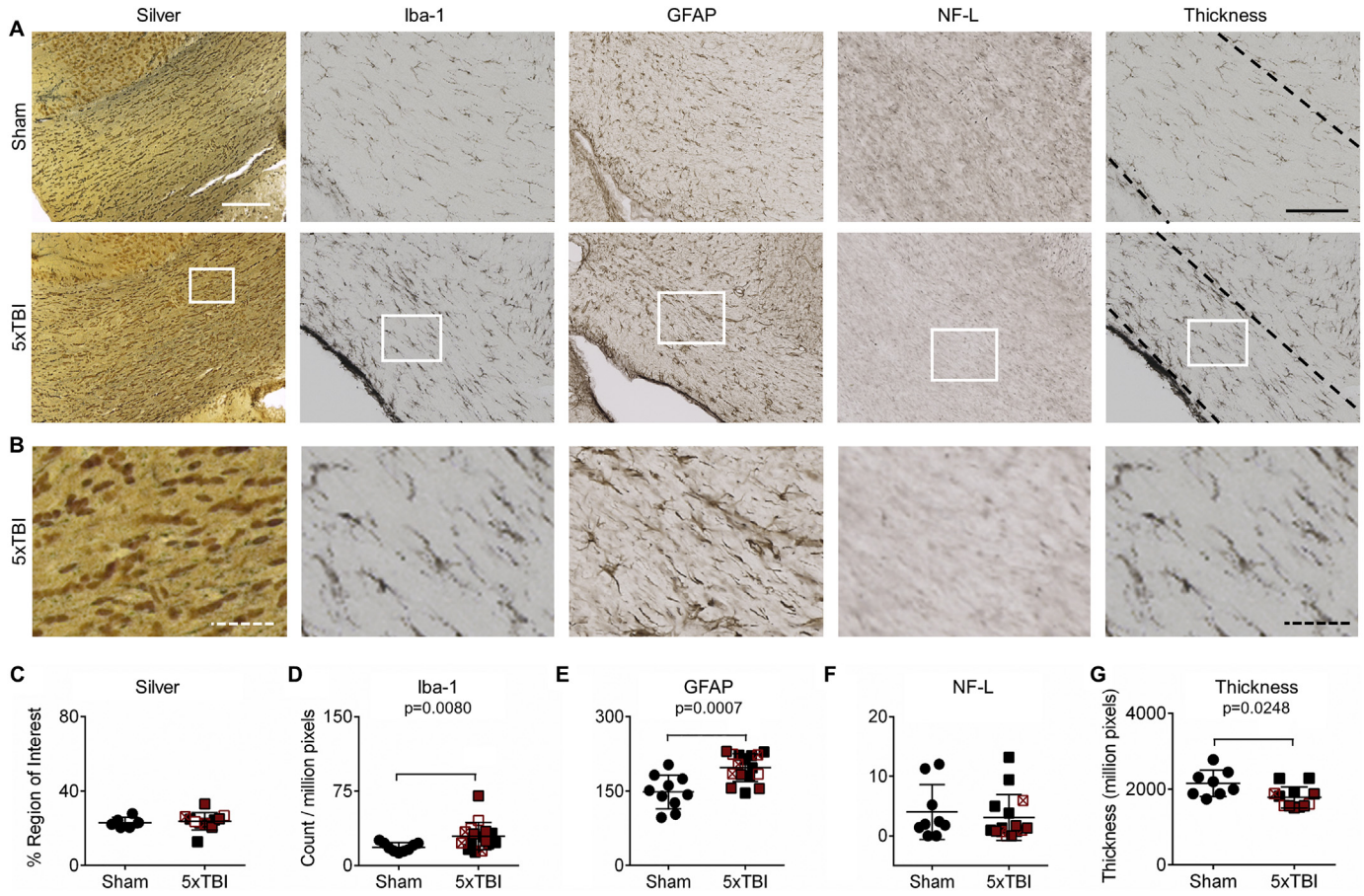

Fig. 4. 5xTBI induces white matter inflammation and degeneration in the corpus callosum. (A) A panel displaying silver, Iba-1, GFAP, and NF-L staining within the corpus callosum at 20× magnification; scale bar = 100 μm. (B) Higher magnification images showing silver, Iba-1, GFAP, and NF-L staining within the corpus callosum following 5xTBI using digital zoom; scale bar = 25 μm. (C) After 5xTBI, the corpus callosum showed no changes in argyrophilic axons. However, (D) activated microglia (Iba-1) were increased following 5xTBI. $p = .0080$. (E) Increased astrogliosis was observed in the corpus callosum following 5xTBI ($p = .0007$) whereas (F) no differences were observed for NF-L positive axonal bulbs (SMI312). (G) There was a significant decrease in thickness of the corpus callosum after 5xTBI ($p = .0248$). In (C-G), TBI samples are colour coded based on performance on the DDT relative to individual baseline: solid black = within baseline; red border, white fill = 1 SD below baseline; red cross = 2 SD below baseline; solid red = 3 SD below baseline. Data are presented as mean ± SD. (For interpretation of the references to colour in this figure legend, the reader is referred to the web version of this article.)

dysfunction in TBI are still relatively unknown, although monoaminergic dysfunction may be a major contributor to impulsive symptoms (Ozga et al., 2018). Data in patients demonstrate enduring dopamine dysfunction, including reduced DAT densities, even when measured many months after injury (Donnemiller et al., 2000; Jenkins et al., 2018). However, in the case of TBI, this dysfunction does not happen in isolation. Notably, the disruption of dopamine pathways may be directly mediated by other pathological factors such as lesion formation and neuroinflammation, and ultimately lead to the emergence of psychiatric symptoms, as well as Parkinsonian-like neurodegeneration (Najjar et al., 2013; Zgaljardic et al., 2015). Given the importance of the mesolimbic circuit in mediating reinforcement-driven behaviors, these dopamine disruptions may reduce capacity for carrying out decisions involving risk and reward, resulting in cognitive impairments.

Despite high clinical relevance, relatively little animal work has focused on the psychiatric aspects of brain injury. In the current study, we measured the effects of repetitive CHIMERA injuries in rats on the DDT, an assessment of trait impulsivity with established translational relevance. While transient changes were observed after a single injury, significant group differences in impulsivity did not emerge until rats were exposed to four or more injuries (Fig. 2A). Studies of human concussion show large individual variability as some patients develop marked deficits (Carroll et al., 2014) while others display relatively minor impairment (Williams et al., 2015; Shultz et al., 2017). Here, we also observed considerable heterogeneity in how individual rats responded to injuries, both behaviorally and neuropathologically. Importantly, measurement of impairment as a function of individual baseline performance across 5 injury cycles allowed us predict the likelihood of mild, moderate, or severe impairment in impulsive decision-making after a given number of TBIs. We determined that 3–4 injuries would be necessary to produce mild impairment in half of our population, whereas 5–6 injuries would be needed for moderate impairment, and 7–8 injuries would be required for severe impairment (Fig. 2F).

Importantly, the current study is the first to demonstrate the effects of successive TBI on impulsive choice in either human or animal settings. However, we have previously reported similar increases in impulsive choice in the CCI model of TBI, a focal means of inducing injury, where impulsivity was increased even with relatively mild focal injury. In contrast to the current data, and possibly due to the open-skull nature of the injury, we also observed cortical inflammation as measured by cytokine elevation in brain homogenate (Vonder Haar et al., 2017). The current study with rat CHIMERA injury suggests a more muted pathological phenotype, with no overt loss of tissue as occurs in focal open-skull models, and selective inflammation as measured by microglia activity in the mesolimbic pathway, potentially owing to the repeat stress of rotational forces inducing axonal shearing. While the pathophysiology of mild TBI is, not surprisingly, subtle, multiple studies

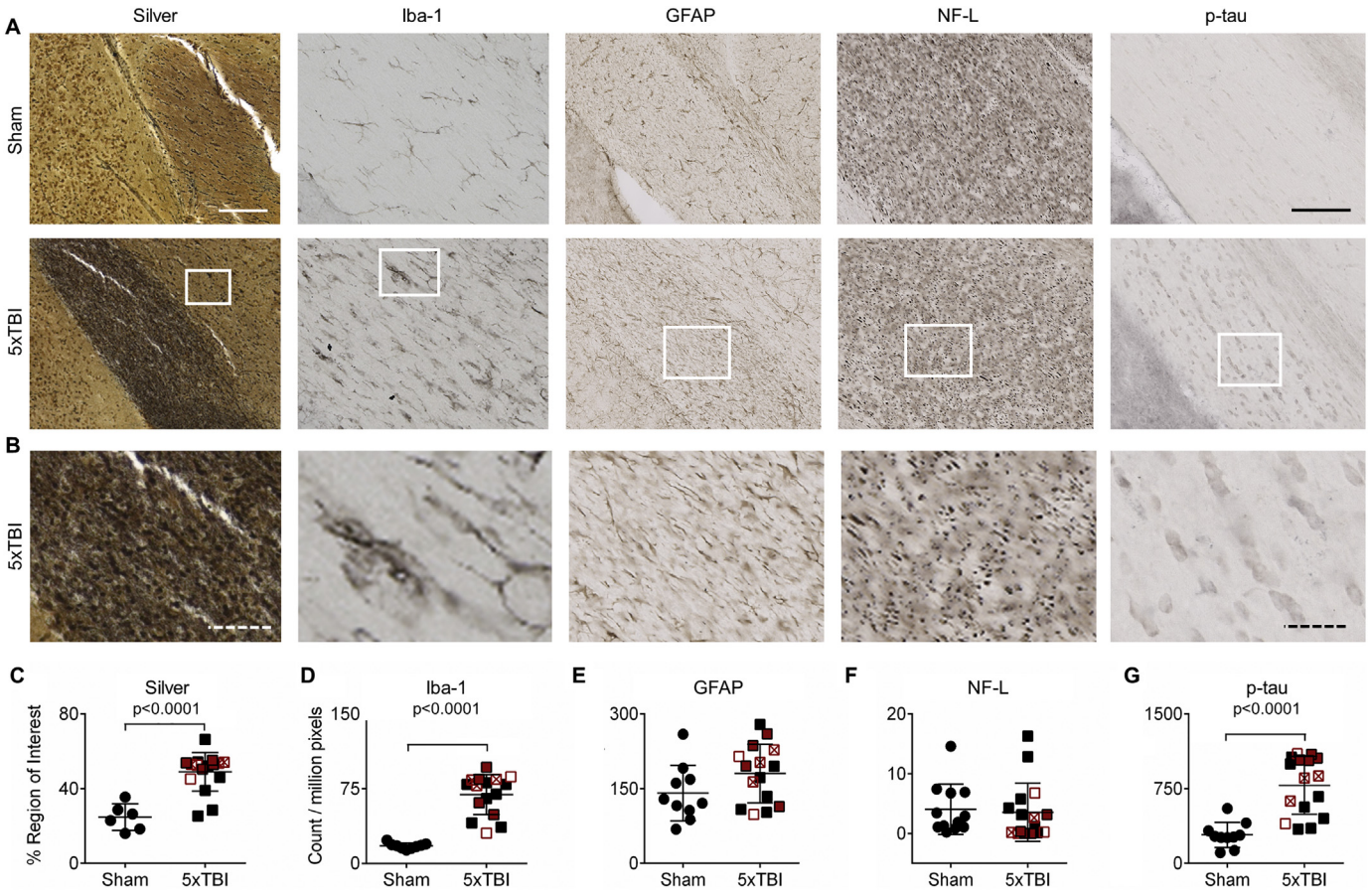

Fig. 5. 5xTBI induces white matter inflammation and degeneration in the optic tract. (A) A panel displaying silver, Iba-1, GFAP, NF-L and p-tau staining within the optic tract imaged at 20× magnification; scale bar = 100 μm. (B) Higher magnification images showing silver, Iba-1, GFAP, NF-L and p-tau staining within the optic tract following 5xTBI using digital zoom; scale bar = 25 μm. (C) After 5xTBI, the optic tract showed increased number of argyrophilic axons (silver; $p < .0001$) and (D) activated microglia (Iba-1; $p < .0001$). (E,F) No differences were observed for GFAP and NF-L positive axonal bulbs (SMI312) in the optic tract. (G) The optic tract showed increased number of p-tau-positive dystrophic axonal punctae (CP13; $p < .0001$). In (C–G), TBI samples are colour coded based on performance on the DDT relative to individual baseline: solid black = within baseline; red border, white fill = 1 SD below baseline; red cross = 2 SD below baseline; solid red = 3 SD below baseline. Data are presented as mean ± SD. (For interpretation of the references to colour in this figure legend, the reader is referred to the web version of this article.)

are beginning to converge upon similar findings. For instance, one recent study examined the ability to inhibit actions (motor impulsivity) after concussive TBI in juvenile rats and found that behavioral disinhibition was increased (albeit, selectively in males) (Hehar et al., 2015). Further, the researchers found pathological features similar to what we report here: alteration of dopamine-related genes (*Comt*, *Drd2*, *Drd3*, *Drd4*, *Maoa*) in the nucleus accumbens and prefrontal cortex as well as changes in dendritic complexity, suggesting alterations to these pathways.

Of particular interest in the current study are the selective alterations to the mesolimbic circuit while sparing the nigrostriatal pathway. Additional studies will be needed to determine the mechanisms that underlie loss of DAT, including loss of the transporter itself, synaptic changes, and axonal damage. Further, the CHIMERA injury settings used here appear to restrict dopaminergic changes to the mesolimibic circuit, which differs from studies using more severe injury models of CCI or fluid percussion injury where significantly decreased TH and DAT in the substantia nigra have been observed (Impellizzeri et al., 2016; Liu et al., 2017). These differences suggest the more subtle nature of the pathology associated with repeated CHIMERA TBI. While dopamine dysfunction may be a proximal cause of impulsive symptoms, our neuropathological analysis showed that repeated CHIMERA TBI resulted in diffuse white matter pathology including axonal damage, microgliosis, astrogliosis, corpus callosum thinning and elevated p-tau immunoreactivity. These observations are consistent with a growing number of rat TBI studies across a wide variety of models. For example, Thomsen et al. observed persistent motor dysfunction, corpus callosum thinning and tauopathy in rats subjected to 5× CCI (Thomsen et al., 2016), which persisted at chronic time points ~8 months post-injury (Thomsen et al., 2017). Using 4× mild lateral fluid percussion injury in rats, Brooks et al. observed inflammation in the ipsilateral corpus callosum, cortex, internal capsule and thalamus that was accompanied by corpus callosum thinning and reduced performance in MWM probe trials (Brooks et al., 2017). Mountey et al. observed sensorimotor dysfunction, prolonged gait abnormalities, inflammation, GFAP, tau, and white matter thinning in rats subjected to repeated noninvasive closed head mTBI (Mountney et al., 2017), whereas Gao et al. observed behavioral dysfunction and activated microglia and GFAP without changes in total or p-tau (ser 202) levels after repetitive mTBI in rats (Gao et al., 2017). Using a modified focal weight drop model with up to 3X TBI spaced 5 days apart, McAteer et al. observed increased tau phosphorylation and microglial activation in the cortex, amyloid precursor protein immunoreactivity, increased escape latency in the Barnes maze and increased anxiety-like behavior (McAteer et al., 2016). Much remains to be learned about how histological changes induced by CHIMERA compare to those of other models, and which of these reflect pathological compared to repair processes.

The approach reported here has several clear advantages over prior

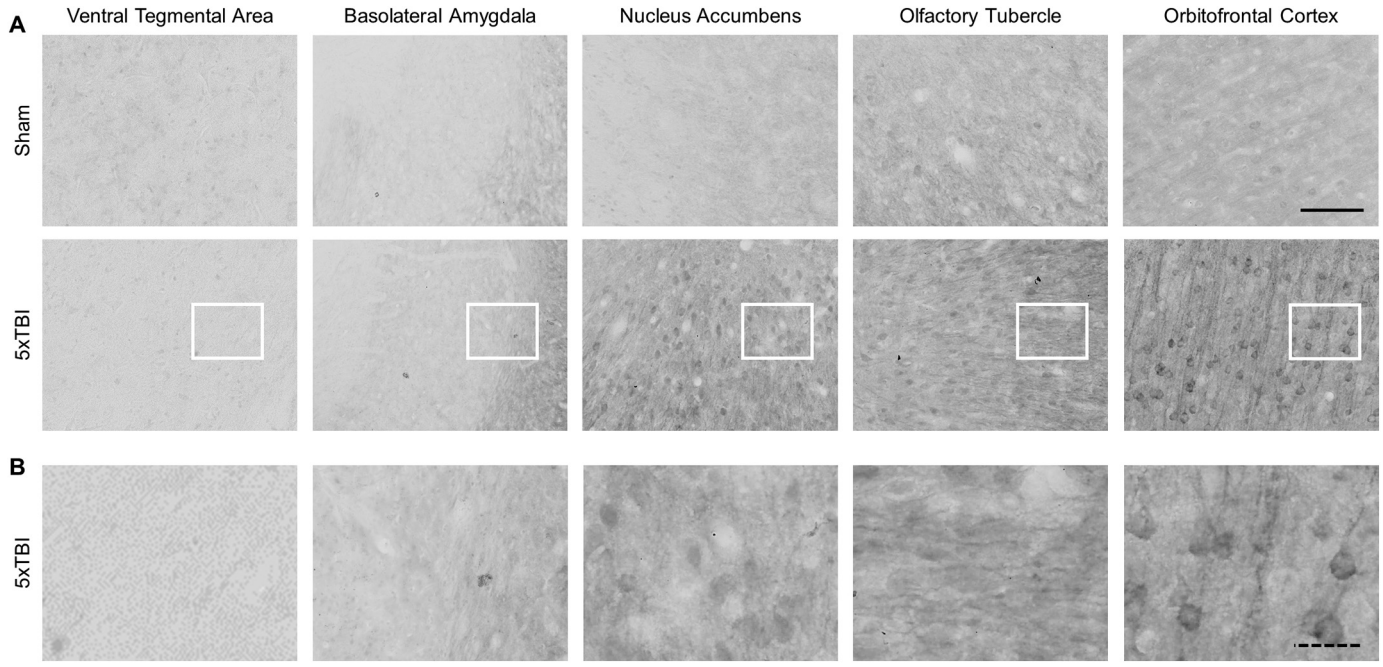

Fig. 6. 5xTBI induces selective changes in p-tau within the mesolimbic pathway. (A) A panel displaying p-tau staining within the mesolimbic system at 20× magnification; scale bar = 100 μm. (B) Higher magnification images showing p-tau staining within the mesolimbic system following 5xTBI using digital zoom; scale bar = 25 μm. After 5xTBI, no qualitative differences in p-tau staining were observed in the ventral tegmental area, basolateral amygdala, and olfactory tubercle. Interestingly, there was a qualitative increase in p-tau staining within the nucleus accumbens shell and orbitofrontal cortex. Quantification was not possible due to strong variations in background stain intensity.

research. The first is the use of CHIMERA to deliver well-controlled repeat injuries. The current iteration of this device includes a two-solenoid design for the release of air pressure to drive the piston, and the venting of air pressure to stabilize the piston after impact. This minimizes inter-operator variability, and provides a reliable (± 2%) impact velocity. Second, the reliability of the injury model is combined with sensitive behavioral testing which can be directly translated into neuropsychological and clinical settings. The DDT in particular has high levels of retest validity, meaning that changes to measured levels of impulsivity are likely to be clinically relevant. Finally, repeated testing with a behavioral assay that is stable across time allowed us to detect relatively subtle effects. One of the largest challenges of studying mild TBI is how to measure what is, by definition, a condition that exerts very minor effects or only affects a subset of individuals (Cassidy et al., 2004). This consideration empowered the generation of predictive models to estimate the likelihood of impairment after a given number of TBIs. Models such as this could be useful, especially when considering questions such as return to play for athletes, return to work for military personnel, or for the inclusion of biomarker data.

As CHIMERA is a relatively new platform to model TBI in multiple animal species, there is as yet no consensus on which criteria should be used to assign injury severity. In mice, we have found that impact energies up to the skull fracture threshold produce surprisingly mild behavioral and neuropathological phenotypes characterized primarily by white matter inflammation (Namjoshi et al., 2014, 2017). In this inaugural rat CHIMERA study, we observed significant mortality and instances of intracranial hemorrhage suggestive of moderate-severe injury even though the LRR data, akin to GSC, did not differ significantly between sham and TBI groups, which is more suggestive of a mild injury. Consistent with the expected phenotype of mild injury, our neuropathological assessment revealed no evidence of gross structural damage or neuronal death, as shown by a lack of significant FluoroJade-C staining (Fig. S4A–B), but indicated consistent diffuse axonal injury and some regions with grey matter inflammation and p-tau deposition. We have therefore refrained from assigning an injury severity to the 5xTBI group.

The study of mTBI is one of the more difficult topics in the field of neurotrauma, with multiple research challenges including selection of injury models, biomarkers, and relevant behavioral assessments. Therefore, it may be beneficial to shift the core question of mTBI from "what are the effects of *X* concussions?" to "how many concussions are necessary for *X* level of dysfunction?" as described herein. This approach may facilitate the identification of biological markers that help identify and predict when an individual is on the cusp of transitioning to impairment as a result of successive injuries. In the current study, we suggest that altered dopamine signaling, combined with white matter neuroinflammation, may be one such marker. Future studies, ideally using a drop-out design including gene expression changes and analyses of neuronal architecture, will be required to fully delineate how altered dopaminergic signaling after repetitive CHIMERA TBI in rats relates to behavioral changes. It will also be important to determine if additional repeated TBIs lead to dysfunction in the nigrostriatal pathway or alter responses to dopaminergic drugs which may be prescribed for both impulsive and motoric dysfunction. As this area is further developed, we may better understand the relationships among head injury exposure, alterations to both neuroinflammatory and dopamine signaling, emergence of psychiatric-like complications, and development of neuropathology including but not limited to findings associated with CTE.

Supplementary data to this article can be found online at https://doi.org/10.1016/j.expneurol.2019.02.012.

Acknowledgements

Operating funding for this work was provided by a Transformational grant from the Weston Brain Institute to CLW (TRA140070), and an internal grant from the Djavad Mowafaghian Centre for Brain Health to CV, KMM, CAW, and CLW. AB was supported by a Canadian Institutes of Health Research Graduate Award and is supported by a University of British Columbia Doctoral Fellowship. CV was supported by a Canadian Institutes of Health Research post-doctoral fellowship. We would like to thank Dr. Haakon Nygaard for use of his confocal microscope and the Canadian Traumatic Brain Injury Research Consortium for constructive

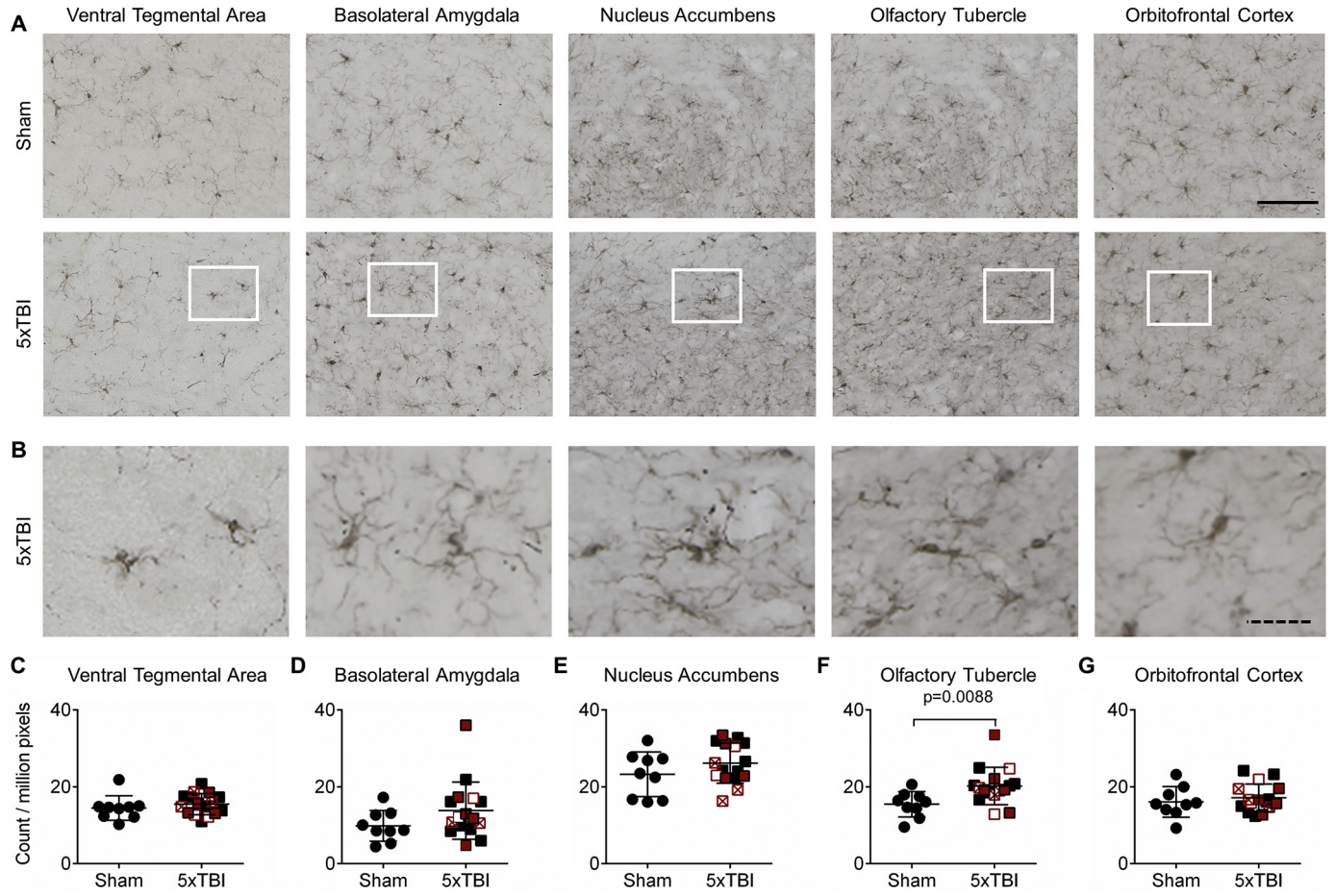

Fig. 7. 5xTBI induces selective changes in microglia within the mesolimbic pathway. (A) A panel displaying Iba-1 staining within the mesolimbic system at 20× magnification; scale bar = 100 μm. (B) Higher magnification images showing Iba-1 staining within the mesolimbic system following 5xTBI using digital zoom; scale bar = 25 μm. (C) After 5xTBI, no differences in Iba-1 staining were observed in the ventral tegmental area, (D) basolateral amygdala, (E) nucleus accumbens shell. (F) Interestingly, there was a significant increase in Iba-1 staining within the olfactory tubercle of the ventral striatum (p = .0088). (G) No differences were observed in the orbitofrontal cortex. In (C–G), TBI samples are colour coded based on performance on the DDT relative to individual baseline: solid black = within baseline; red border, white fill = 1 SD below baseline; red cross = 2 SD below baseline; solid red = 3 SD below baseline. Data are presented as mean ± SD. (For interpretation of the references to colour in this figure legend, the reader is referred to the web version of this article.)

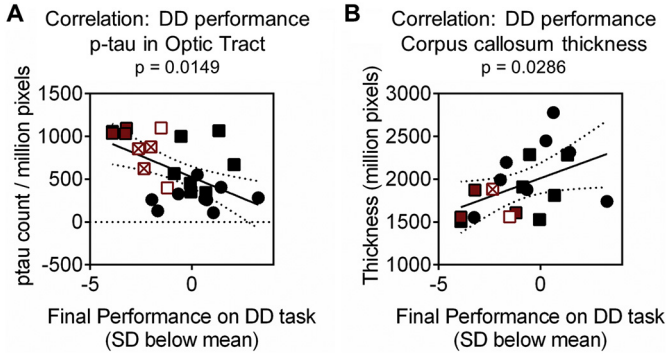

Fig. 8. Correlations between DDT performance and neuropathology. (A) Pearson correlations were calculated for sham and 5xTBI data extracted from final performance on delay discounting task and p-tau quantification in optic tract. The negative correlation reached significance (r = −0.5496, p = .0036). (B) The positive correlation between sham and 5xTBI data extracted from final performance on delay discounting task and corpus callosum thickness was also significant (r = 0.4647, p = .0450). In (A–B) TBI samples are colour coded based on performance on the DDT relative to individual baseline: solid black square = within baseline; red border, white fill = 1 SD below baseline; red cross = 2 SD below baseline; solid red = 3 SD below baseline. Sham samples: solid black circle. (For interpretation of the references to colour in this figure legend, the reader is referred to the web version of this article.)

feedback.

Competing interests

In the past three years, CAW has been a member of an Advisory Board for Shire Pharmaceuticals with reference to an unrelated matter. CLW had previous sponsored research projects with AstraZeneca and Pfizer on unrelated topics. The authors have no other financial disclosures or potential conflicts of interest to declare.

References

Arnould, A., et al., 2016. Neurobehavioral and self-awareness changes after traumatic brain injury: towards new multidimensional approaches. Ann. Phys. Rehabil. Med 59 (1), 18–22. https://doi.org/10.1016/j.rehab.2015.09.002.

Baik, J.-H., 2013. Dopamine Signaling in reward-related behaviors. Front. Neural Circ 7. https://doi.org/10.3389/fncir.2013.00152.

Bailey, M.R., Simpson, E.H., Balsam, P.D., 2016. Neural substrates underlying effort, time, and risk-based decision making in motivated behavior. Neurobiol. Learn. Mem. 133, 233–256. https://doi.org/10.1016/j.nlm.2016.07.015.

Bales, J.W., et al., 2009. Persistent cognitive dysfunction after traumatic brain injury: a dopamine hypothesis. Neurosci. Biobehav. Rev. 33 (7), 981–1003. https://doi.org/10.1016/j.neubiorev.2009.03.011.

Banks, S.J., et al., 2014. Impulsiveness in professional fighters. J. Neuropsychiatry Clin. Neurosci 26 (1), 44–50. https://doi.org/10.1176/appi.neuropsych.12070185.

Bjork, J.M., et al., 2016. Laboratory impulsivity and depression in blast-exposed military personnel with post-concussion syndrome. Psychiatry Res. 246, 321–325. https://doi.org/10.1016/j.psychres.2016.10.008.

Bjork, J.M., et al., 2017. Rapid-response impulsivity predicts depression and posttraumatic stress disorder symptomatology at 1-year follow-up in blast-exposed service members. Arch. Phys. Med. Rehabil. 98 (8), 1646–1651. https://doi.org/10.1016/j.apmr.2017.03.022.

Brewer, J.A., Potenza, M.N., 2008. The neurobiology and genetics of impulse control disorders: relationships to drug addictions. Biochem. Pharmacol. 75 (1), 63–75. https://doi.org/10.1016/j.bcp.2007.06.043.

Brooks, D.M., et al., 2017. Multiple mild traumatic brain injury in the rat produces persistent pathological alterations in the brain. Exp. Neurol. 297, 62–72. https://doi.org/10.1016/j.expneurol.2017.07.015.

Broshek, D.K., De Marco, A.P., Freeman, J.R., 2015. A review of post-concussion syndrome and psychological factors associated with concussion. Brain Inj. 29 (2), 228–237. https://doi.org/10.3109/02699052.2014.974674.

Carroll, L.J., et al., 2014. Systematic review of the prognosis after mild traumatic brain injury in adults: cognitive, psychiatric, and mortality outcomes: results of the international collaboration on mild traumatic brain injury prognosis. Arch. Phys. Med. Rehabil. 95 (3). https://doi.org/10.1016/j.apmr.2013.08.300.

Cassidy, J.D., et al., 2004. Incidence, risk factors and prevention of mild traumatic brain injury: results of the WHO collaborating centre task force on mild traumatic brain injury. J. Rehabil. Med. 43, 28–60. https://doi.org/10.1080/16501960410023732.

Chen, Y.-H., et al., 2017. Impact of traumatic brain injury on dopaminergic transmission. Cell Transplant. 26 (7), 1156–1168. https://doi.org/10.1177/0963689717714105.

Clark, L., Cools, R., Robbins, T.W., 2004. The neuropsychology of ventral prefrontal cortex: decision-making and reversal learning. Brain Cogn. 55 (1), 41–53. https://doi.org/10.1016/S0278-2626(03)00284-7.

Dixon, M.R., et al., 2005. Impulsivity, self-control, and delay discounting in persons with acquired brain injury. Behav. Interv. 20 (1), 101–120. https://doi.org/10.1002/bin.173.

Donnell, A.J., et al., 2012. Incidence of postconcussion symptoms in psychiatric diagnostic groups, mild traumatic brain injury, and comorbid conditions. Clin. Neuropsychol. 26 (7), 1092–1101. https://doi.org/10.1080/13854046.2012.713984.

Donnemiller, E., et al., 2000. Impaired dopaminergic neurotransmission in patients with traumatic brain injury: a SPET study using 123I-beta-CIT and 123I-IBZM. Eur. J. Nucl. Med. 27, 1410–1414. https://doi.org/10.1007/s002590000308.

Frieden, T.R., Houry, D., Baldwin, G., 2015. Traumatic brain injury in the United States: epidemiology and rehabilitation. CDC NIH Rep. Congr 1–74. https://doi.org/10.3171/2009.10.JNS091500.

Gao, H., et al., 2017. The accumulation of brain injury leads to severe neuropathological and neurobehavioral changes after repetitive mild traumatic brain injury. Brain Res. 1657, 1–8. https://doi.org/10.1016/j.brainres.2016.11.028.

Goswami, R., et al., 2016. Frontotemporal correlates of impulsivity and machine learning in retired professional athletes with a history of multiple concussions. Brain Struct. Funct. 221 (4), 1911–1925. https://doi.org/10.1007/s00429-015-1012-0.

Graham, D.P., Cardon, A.L., 2008. An update on substance use and treatment following traumatic brain injury. Ann. N. Y. Acad. Sci. 1141, 148–162. https://doi.org/10.1196/annals.1441.029.

Hehar, H., et al., 2015. Impulsivity and concussion in juvenile rats: examining molecular and structural aspects of the frontostriatal pathway. PLoS One 10 (10), 1–24. https://doi.org/10.1371/journal.pone.0139842.

Hodel, A.S., et al., 2016. Hot executive function following moderate-to-late preterm birth: altered delay discounting at 4 years of age. Dev. Sci. 19 (2), 221–234. https://doi.org/10.1111/desc.12307.

Hyder, A.A., et al., 2007. The impact of traumatic brain injuries: A global perspective. NeuroRehabilitation 22, 341–353. http://iospress.metapress.com/content/103177/?sortorder=asc.

Impellizzeri, D., et al., 2016. Traumatic brain injury leads to development of Parkinson's disease related pathology in mice. Front. Neurosci. 10, 1–13. https://doi.org/10.3389/fnins.2016.00458.

Iverson, G.L., et al., 2018. The need to separate chronic traumatic encephalopathy neuropathology from clinical features. 61, 17–28. https://doi.org/10.3233/JAD-170654.

Jenkins, P.O., et al., 2018. Dopaminergic abnormalities following traumatic brain injury. Brain 141 (3), 797–810. https://doi.org/10.1093/brain/awx357.

Kim, E., 2002. Agitation, aggression, and disinhibitionsyndromes after traumatic brain injury. NeuroRehabilitation 17, 297–310.

Kocka, A., Gagnon, J., 2014. Definition of impulsivity and related terms following traumatic brain injury: a review of the different concepts and measures used to assess impulsivity, disinhibition and other related concepts. Behav. Sci. 4, 352–370. https://doi.org/10.3390/bs4040352.

Liu, M., et al., 2017. Pioglitazone attenuates neuroinflammation and promotes dopaminergic neuronal survival in the nigrostriatal system of rats after diffuse brain injury. J. Neurotrauma 34 (2), 414–422. https://doi.org/10.1089/neu.2015.4361.

Mahar, I., Alosco, M.L., McKee, A.C., 2017. Psychiatric phenotypes in chronic traumatic encephalopathy. Neurosci. Biobehav. Rev. 83, 622–630. https://doi.org/10.1016/j.neubiorev.2017.08.023.

McAteer, K.M., et al., 2016. Short and long term behavioral and pathological changes in a novel rodent model of repetitive mild traumatic brain injury. PLoS One 11 (8), 1–18. https://doi.org/10.1371/journal.pone.0160220.

McKee, A.C., Daneshvar, D.H., 2015. The neuropathology of traumatic brain injury. Handb. Clin. Neurol. 127, 45–66. https://doi.org/10.1016/B978-0-444-52892-6.00004-0.The.

McKee, A.C., et al., 2016. The first NINDS/NIBIB consensus meeting to define neuropathological criteria for the diagnosis of chronic traumatic encephalopathy. Acta Neuropathol. 131 (1), 75–86. https://doi.org/10.1007/s00401-015-1515-z.

Merkel, S.F., et al., 2017. Factors affecting increased risk for substance use disorders following traumatic brain injury: what we can learn from animal models. Neurosci. Biobehav. Rev. 77, 209–218. https://doi.org/10.1016/j.neubiorev.2017.03.015.

Mez, J., et al., 2017. Clinicopathological evaluation of chronic traumatic encephalopathy in players of American football. JAMA J. Am. Med. Assoc 318 (4), 360–370. https://doi.org/10.1001/jama.2017.8334.

Mountney, A., et al., 2017. Functional and molecular correlates after single and repeated rat closed-head concussion: indices of vulnerability after brain injury. J. Neurotrauma. https://doi.org/10.1089/neu.2016.4679. 2789, p. neu.2016.4679.

Myerson, J., Green, L., Warusawitharana, M., 2001. Area under the curve as a measure of discounting. J. Exp. Anal. Behav. 76 (2), 235–243. https://doi.org/10.1901/jeab.2001.76-235.

Najjar, S., et al., 2013. Neuroinflammation and psychiatric illness. J. Neuroinflammation 10. https://doi.org/10.1186/1742-2094-10-43.

Namjoshi, D.R., et al., 2013. The liver X receptor agonist GW3965 improves recovery from mild repetitive traumatic brain injury in mice partly through Apolipoprotein E. PLoS One 8 (1). https://doi.org/10.1371/journal.pone.0053529.

Namjoshi, D.R., et al., 2014. Merging pathology with biomechanics using CHIMERA (closed-head impact model of engineered rotational acceleration): a novel, surgery-free model of traumatic brain injury. Mol. Neurodegener. 9, 55. https://doi.org/10.1186/1750-1326-9-55.

Namjoshi, D.R., et al., 2017. Defining the biomechanical and biological threshold of murine mild traumatic brain injury using CHIMERA (closed head impact model of engineered rotational acceleration). Exp. Neurol. 292, 80–91. https://doi.org/10.1016/j.expneurol.2017.03.003.

Ozga, J.E., et al., 2018. Executive (dys)function after traumatic brain injury. Behav. Pharmacol 1. https://doi.org/10.1097/FBP.0000000000000430.

Rizzi, G., Tan, K.R., 2017. Dopamine and acetylcholine, a circuit point of view in Parkinson's disease. Front. Neural Circ 11. https://doi.org/10.3389/fncir.2017.00110.

Rochat, L., et al., 2010. Assessment of impulsivity after moderate to severe traumatic brain injury. Neuropsychol. Rehabil 20 (5), 778–797. https://doi.org/10.1080/09602011.2010.495245.

Schwarzbold, M., et al., 2008. Psychiatric disorders and traumatic brain injury. Neuropsychiatr. Dis. Treat. 4 (4), 797–816. https://doi.org/10.2147/NDT.S2653.

Shultz, S.R., et al., 2017. The potential for animal models to provide insight into mild traumatic brain injury: translational challenges and strategies. Neurosci. Biobehav. Rev. 76, 396–414. https://doi.org/10.1016/j.neubiorev.2016.09.014.

Thomsen, G.M., et al., 2016. A model of recurrent concussion that leads to long-term motor deficits, CTE-like tauopathy and exacerbation of an ALS phenotype. J. Trauma Acute Care Surg. 81 (6), 1070–1078. https://doi.org/10.1097/TA.0000000000001248.

Thomsen, G.M., et al., 2017. Clinical correlates to assist with chronic traumatic encephalopathy diagnosis: insights from a novel rodent repeat concussion model. J. Trauma Acute Care Surg. 82 (6), 1039–1048. https://doi.org/10.1097/TA.0000000000001443.

Vonder Haar, C., et al., 2016. Frontal traumatic brain injury in rats causes long-lasting impairments in impulse control that are differentially sensitive to pharmacotherapeutics and associated with chronic neuroinflammation. ACS Chem. Neurosci. 7 (11), 1531–1542. https://doi.org/10.1021/acschemneuro.6b00166.

Vonder Haar, C., et al., 2017. Frontal traumatic brain injury increases impulsive decision making in rats: a potential role for the inflammatory cytokine Interleukin-12. J. Neurotrauma 34 (19), 2790–2800. https://doi.org/10.1089/neu.2016.4813.

Wagner, A.K., et al., 2014. The influence of genetic variants on striatal dopamine transporter and D2 receptor binding after TBI. J. Cereb. Blood Flow Metab. 34 (8), 1328–1339. https://doi.org/10.1038/jcbfm.2014.87.

Weafer, J., Baggott, M.J., De Wit, H., 2013. Test-retest reliability of behavioral measures of impulsive choice, impulsive action, and inattention. Exp. Clin. Psychopharmacol. 21 (6), 475–481. https://doi.org/10.1037/a0033659.

Weil, Z.M., Karelina, K., 2017. Traumatic brain injuries during development: implications for alcohol abuse. Front. Behav. Neurosci. 11 (July), 1–8. https://doi.org/10.3389/fnbeh.2017.00135.

Wilk, J.E., et al., 2012. Mild traumatic brain injury (concussion), posttraumatic stress disorder, and depression in U.S. soldiers involved in combat deployments: association with postdeployment symptoms. Psychosom. Med. 74 (3), 249–257. https://doi.org/10.1097/PSY.0b013e318244c604.

Williams, R.M., et al., 2015. Concussion recovery time among high school and collegiate athletes: a systematic review and meta-analysis. Sports Med. 45 (6), 893–903. https://doi.org/10.1007/s40279-015-0325-8.

Winstanley, C.A., 2007. The orbitofrontal cortex, impulsivity, and addiction. Ann. N. Y. Acad. Sci. 1121 (604), 639–655. https://doi.org/10.1196/annals.1401.024.

Winstanley, C.A., 2010. The neural and neurochemical basis of delay discounting. In: Impulsivity: The Behavioral and Neurological Science of Discounting. American Psychological Association, Washington, DC, US, pp. 95–121. https://doi.org/10.1037/12069-004.

Winstanley, C.A., Eagle, D.M., Robbins, T.W., 2006. Behavioral models of impulsivity in relation to ADHD: translation between clinical and preclinical studies. Clin. Psychol. Rev. 26 (4), 379–395. https://doi.org/10.1016/j.cpr.2006.01.001.

Zgaljardic, D.J., et al., 2015. Psychiatric disease and post-acute traumatic brain injury. J. Neurotrauma 32 (23), 1911–1925. https://doi.org/10.1089/neu.2014.3569.